
Proceedings Paper:
Meza, F. and Becque, J. (2017) 07.15: Experimental and numerical investigation of cold-formed steel built-up stub columns. In: Ce/Papers. Eurosteel 2017, 13-15 Sep 2017, Copenhagen, Denmark. Ernst & Sohn Verlag , pp. 1617-1626.

https://doi.org/10.1002/cepa.205

Experimental and numerical investigation of cold-formed steel built-up stub columns

Francisco Meza[a], Jurgen Becque*,[a]

[a]The University of Sheffield, Dept. Civil and Structural Engineering, UK
fjmezaortiz1@sheffield.ac.uk, j.becque@sheffield.ac.uk

ABSTRACT

This paper describes a numerical and experimental programme carried out at the University of Sheffield on built-up stub columns fabricated from cold-formed steel. A total of 20 built-up columns with four different cross-sectional geometries were tested between fixed end conditions. Two of the cross-sectional geometries were assembled using M6 bolts and the other two using M5.5 self-drilling sheet metal screws. The connector spacing was varied among specimens of the same cross-sectional geometry. The cross-sections were assembled from flat plate, plain channels and lipped channels with nominal thicknesses ranging from 1.2 mm to 2.4 mm. The initial geometric imperfections of each specimen were recorded prior to testing and their material properties were determined by means of tensile coupon tests. Single lap shear tests were also carried out in order to study the connector behaviour of the bolts and the screws used to assemble the specimens.
As part of the numerical part of the study, the test specimens were modelled using the commercially available ABAQUS software package. The recorded geometric imperfections, the measured material properties and the connector behaviour data obtained from the lap shear tests were incorporated into the FE models. Special attention was paid to the connector modelling in order to find an effective and simple way to represent their actual behaviour. The FE models were further used to quantify the effect of the connector behaviour on the buckling response of cold-formed steel built-up stub columns.

Keywords: Built-up column, Cross-sectional capacity, Axial compression, Cold-formed steel

1 INTRODUCTION

Cold-formed steel (CFS) offers a number of advantages compared to traditional hot-rolled steel. For example, they possess a high strength-to-weight ratio, are produced by a relatively simple manufacturing process and are easy to handle, stack and transport, allowing for high speeds of construction. Therefore, they are experiencing a rapid widening in their range of applications, having evolved from primarily being used as secondary members to increasingly forming part of the main load-bearing structure. Examples of this evolution are multi-storey buildings [1] and portal frames [2] constructed entirely out of cold-formed steel. This trend in construction is putting an increased demand on the cold-formed steel industry to produce sections that can resist higher loads and cover longer spans. A relatively straightforward way to meet these new demands is to use the already commercially available CFS sections to assemble built-up sections using mechanical fasteners. However, a lack of understanding of the way these built-up sections behave and a gap in specific design provisions prevent the exploitation of the real potential of these types of sections. The buckling response of built-up members is potentially affected by the specific characteristics of the type of connectors used for the assemblage, as well as their spacing, as these are likely to affect the degree to which the individual components work as one cross-section and the way they interact with each other as they buckle.
A number of experiments have previously been carried out on built-up sections in order to shed light on the way these sections behave. In [3, 4] a series of compressive tests were carried out on closed and open built-up columns consisting of two sigma sections connected with screws. The typical I-section made up of two lipped channels connected back-to-back has been extensively

studied, in [5, 6] where the components were connected using sheet metal screws, and in [7–9] where the channels were welded together. A double-Z built-up member connected with bolts has also been studied in [10], both in compression and in bending. It should be noted that all these tests have only accounted for built-up sections made of two identical components, in which both components buckle at the same time.

An experimental and numerical programme of 20 CFS built-up stub columns with four different cross-sectional geometries is presented in this paper. The specimens were assembled using either screws or bolts, placed at spacings which varied among specimens. They were subjected to compression between fixed end conditions. In addition, the material properties and the initial geometric imperfections of the built-up specimens, as well as the mechanical behaviour of the connectors were determined experimentally. The test specimens were modelled using ABAQUS and the results were compared to the experiment. Good agreement was achieved between the FE models and the experimental results. The FE models were further used to evaluate the effect of different connector models and connector behaviour on the buckling response of CFS built-up stub columns.

2 SPECIMEN GEOMETRY

Four different cross-sectional geometries were tested as part of the experimental programme, as illustrated in *Fig.1*. All built-up specimens were designed to fail by cross sectional buckling, excluding global instability. *Table 1* lists the nominal dimensions of the components used to assemble each built-up geometry. The length of the specimens was chosen to accommodate at least three local or distortional buckle half-waves. As a result, columns with built-up geometries 1, 3 and 4 were given a length of 1100 mm and columns with built-up geometry 2 had a length of 800 mm. Specimens with built-up geometries 1 and 2 were assembled using M6 bolts and were tested with three different connector spacings. More specifically, 2, 3 or 5 equally spaced connectors were used for geometry 1, and 2, 4 or 6 connectors were chosen for geometry 2. Specimens with built-up geometries 3 and 4, on the other hand, were assembled using M5.5 self-drilling screws and were tested with either 2 or 5 equally spaced connectors.

Each of the built-up geometries was labelled using the letters '*SC*' and the number 1 to 4, to indicate the cross-sectional configuration (with reference to *Fig. 1*), followed by the number of rows of intermediate connectors (i.e. not counting the connectors at the end sections). Since each test was repeated, the letters '*a*' and '*b*' were used to indicate whether the specimen was the first or the second of twin column tested. To refer to the individual components used to assemble the built-up columns, the letters '*T*' '*S*' or '*P*' were used to indicate whether the component was a plain channel, a lipped channel or a plate. This was followed by the nominal width of the web of the channel (or the width of the plate) in mm and the nominal thickness of the section in mm multiplied by 10.

Table 1. Nominal dimensions of the components (mm)

Column	section	Web/Plate Width	Flange	Lip	Thickness
SC1	T15414	154	54	-	1.4
	P20024	200	-	-	2.4
SC2	T15414	154	54	-	1.4
	T7912	79	36	-	1.2
SC3/SC4	T12012	120	40	-	1.2
	S11012	110	50	10	1.2

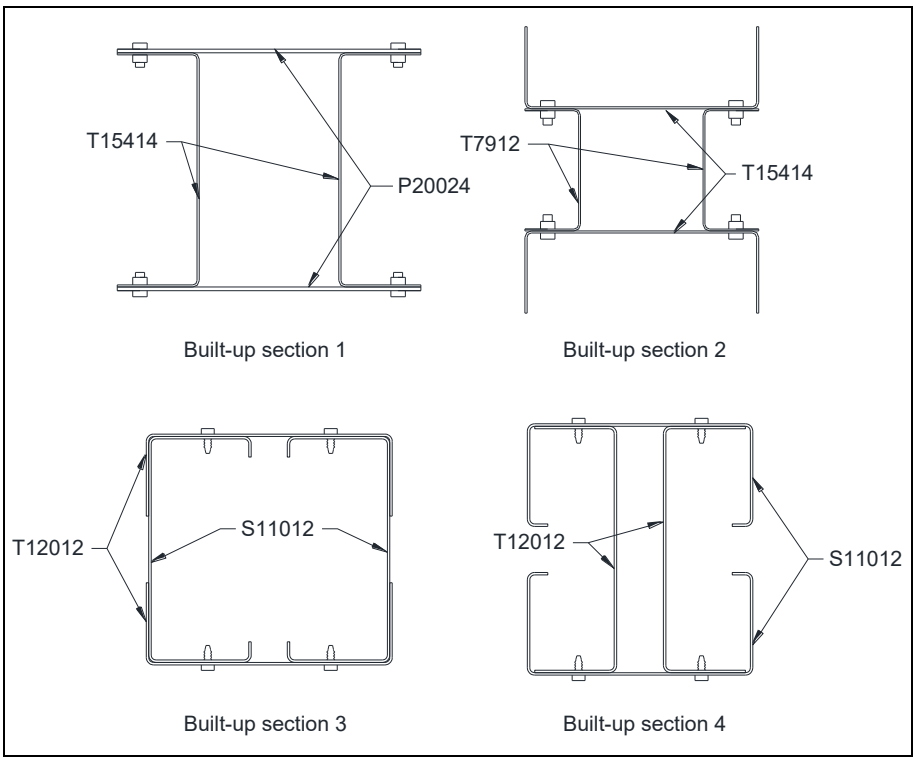

Fig. 1. Built-up cross-sectional geometries

3 MATERIAL PROPERTIES

A series of tensile coupons tests was carried out in order to determine the material properties of the test specimens. The coupons were cut from spare sections belonging to the same batch as those used in the test and were taken in the longitudinal (rolling) direction of the specimen. Two flat coupons were taken along the centre line of the web of each type of channel and along the centre line of the plate section. Two corner coupons were also taken from the web-flange junctions of each type of channel in order to determine the effect of the cold-working process on the material properties.
Fig. 2 shows the set-up used to carry out the tensile coupon tests. The flat coupons had a nominal width of 12.5 mm and each of them was instrumented with an extensometer and two strain gauges, one on each side of the coupon. The corner coupons had a nominal width of 6 mm and were tested in pairs to avoid introducing unwanted bending moments due to their asymmetric cross-sectional shape. Each pair of corner coupons was instrumented with an extensometer and a strain gauge attached to the outside of each coupon.

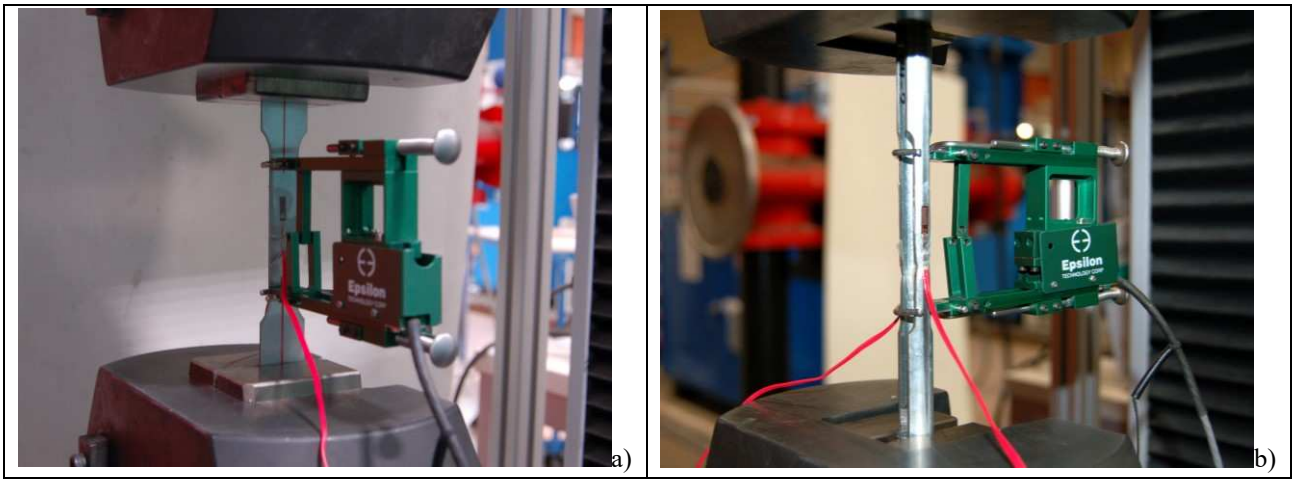

Fig. 2. a) Flat coupon; b) Corner coupon

All coupons were tested following the specifications given in the relevant European standard [11]. *Table 2* lists the average values of the Young's modulus (E), the 0.2% proof stress ($\sigma_{0.2\%}$) and the tensile strength (σ_u) obtained for each pair of twin coupons.

Table 2. Material properties of tensile coupons

Type	Section	E (GPa)	$\sigma_{0.2\%}$ (MPa)	σ_u (MPa)
Flat	P20024	195	437	519
Flat	T15414	207	609	705
Flat	T7912	195	419	537
Flat	T12012	192	242	320
Flat	S11012	198	277	357
Corner	T15414	231	617	733
Corner	T7912	217	487	605
Corner	T12012	231	305	351
Corner	S11012	253	340	383

4 MEASUREMENT OF GEOMETRIC IMPERFECTIONS

Geometric imperfections may significantly affect the stability of thin-walled CFS members, especially when coupled instabilities are involved. For this reason, the magnitude and shape of the imperfections of each specimen were recorded before testing. The measurements were performed after the built-up columns were assembled into their final configurations, as joining the single sections together might somewhat modify their geometric imperfections.

The out-of-plane imperfections were recorded using the set-up described in [12], in which two electric motors were used to move a laser sensor along high-precision bars, mounted on top of a flat table. The table provided a flat surface with a deviation from flatness of less than 0.06 mm and was used as a reference for the measurements. The laser sensor was used to take readings along different longitudinal lines on each side of the built-up specimens, as shown in *Fig. 3*. Imperfections were measured along the center line and both edges of the webs of the channels, the plate sections and the flanges of the lipped channels. In order to introduce these imperfections into the FE model, the imperfections at intermediate points within the cross-section were obtained using second order polynomial interpolation. For the flanges of the plain channels, imperfections were recorded along the web-flange corner and the flange tip. Imperfection values along the flange were then obtained using linear interpolation.

The imperfections of some plate elements could not be recorded after the specimens were assembled due to lack of physical space to position the laser sensor. If this was the case and the imperfection was nevertheless thought to be of importance (because the component constituted the most slender part of the cross-section), the imperfections were recorded before assembling the cross-section.

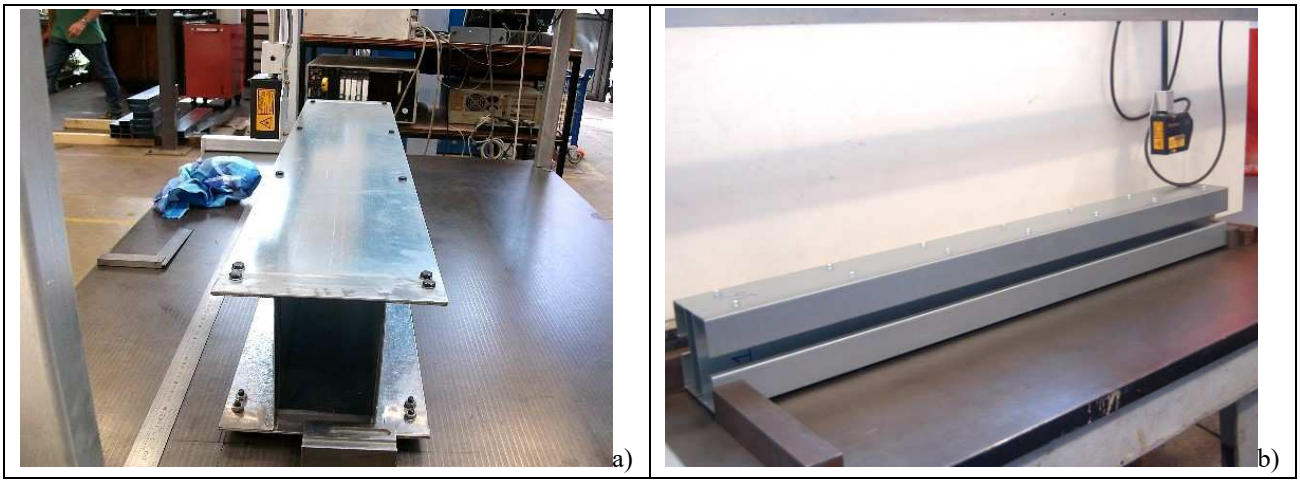

Fig. 3. Measurement of geometric imperfections of a) SC1; b) SC4

5 TEST SET-UP

All specimens were tested between fixed end supports. Two LVDTs were used to record the axial shortening of the specimens and monitor that no rotation occurred at the top end of the specimen. Readings obtained from both of these LVDTs were in close agreement for all specimens. In addition, for specimens SC1 and SC2 twelve potentiometers, divided over two cross-sections and placed at mid-distance between connectors, were used to measure the out-of-plane deformations of the components and capture the onset of local buckling. For specimens SC3 and SC4 eight and ten potentiometers, respectively, were placed at two different heights in order to capture the onset of cross-sectional buckling. The eight potentiometers were placed at mid-distance between the connectors of specimens SC3, while for specimens SC4 five potentiometers were placed at mid-distance between connectors and the other five potentiometers were placed within a cross-section containing connectors.

The specimens were tested in an ESH universal testing machine with a capacity of 1000 kN. The tests were carried out at a strain rate of 1.7×10^{-6} /s for all specimens, resulting in a displacement rate of 0.11 mm/min for specimens SC1, SC3 and SC4 (with a length of 1100 mm) and 0.08 mm/min for specimens SC2 (with a length of 800 mm).

6 TEST RESULT

All built-up columns failed due to cross-sectional buckling, displaying significant interaction between the components in the process. *Fig. 4* shows the load vs. axial displacement curves of all the specimens. In general, good agreement in the ultimate load was obtained within each pair of twin specimens, with a maximum difference of 8.97 %, 6.28 %, 2.73 % and 2.03 % for specimens SC1, SC2, SC3 and SC4, respectively.

The tests also show a modest increment in the ultimate load for built-up specimens SC1 as the connector spacing is reduced. More specifically, increasing the number of connectors from 2 to 5 produced an increase in the ultimate load of 10.81 %. In the case of built-up specimens SC2, the tests show that increasing the number of connectors does not necessarily result in a noticeable increase of the ultimate load. For example, columns SC2-4 showed a comparable (and actually slightly higher) ultimate load relative to columns SC2-6. Looking at built-up specimens SC3 and SC4, increasing the number of connectors from 2 to 5 resulted in a marginal increase in the ultimate load of 1.20 % for the former and a reduction in the ultimate load of 4.74 % for the latter.

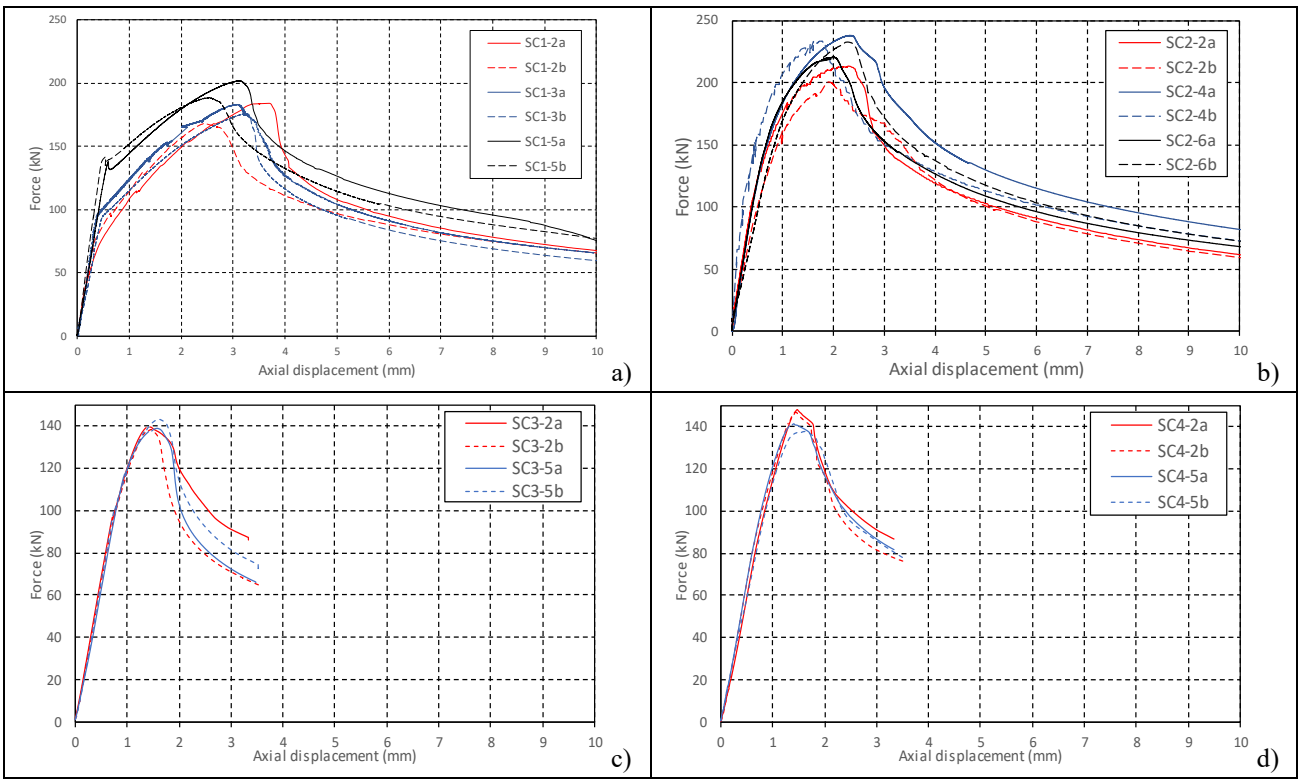

Fig. 4. Axial load vs axial deformation curve for a) SC1; b) SC2; c) SC3; d) SC4

7 SINGLE LAP SHEAR TESTS

The connectors used to assemble the built-up columns were tested using a conventional single lap shear test configuration with two fasteners in the line of stress. The specimens were fabricated from steel strips taken from spare sections of the built-up columns. Three types of specimens were fabricated to cover the combinations of ply thicknesses and fastener types encountered in the built-up columns. Two identical specimens were fabricated for each configuration in order to account for statistical variability in the results. The dimensions of the connector test specimens were chosen following the recommendations given in [13] and they were assembled, as much as possible, in the same way as the built-up specimens (for instance, applying the same torque on the bolts).

The label used to refer to the connector test specimens consists of the letters '*CB*' or '*CS*' to indicate whether the specimen was assembled using bolts or screws, respectively, followed by the thickness in mm of the fastened steel plates multiplied by 10.

All connector specimens were tested in a 300 kN Shimadzu universal testing machine and were loaded until failure at a displacement rate of 0.5 mm/min.

Fig. 5 shows the average results obtained from the bolted specimens corresponding to built-up columns SC1 and SC2, and the screwed specimens corresponding to built-up columns SC3 and SC4.

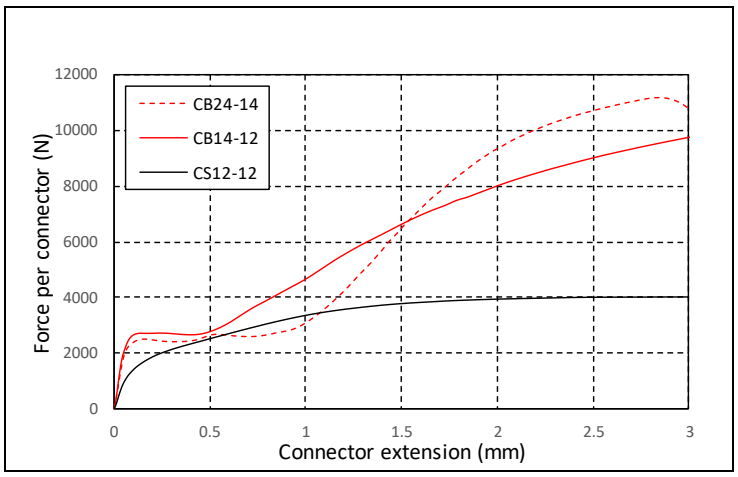

Fig. 5. Load-extension behaviour of connector test specimens

8 FE MODEL

FE models of all built-up stub column tests were developed using the ABAQUS software. The component channels and plates of the built-up specimens were modelled using S4R5 shell elements.

8.1 Material properties and geometrical imperfections

The material properties of the steel sheets were modelled as elastic-plastic, using isotropic linear elastic material behaviour combined with the standard metal plasticity model available in ABAQUS. Different material properties were assigned to the flat portions and the corner regions. The elastic behaviour was defined using a Poisson's ratio of 0.3 and the elastic modulus obtained from the tensile coupons. The tensile coupon results were also used to define the inelastic material behaviour, after the engineering stresses and strains were converted into true stresses and logarithmic plastic strains.

The initial geometric imperfections measured on the test specimens were introduced in the FE model by modifying the initial coordinates of the nodes in the input file (*.inp) of a geometrically perfect FE model generated in ABAQUS. This was carried out using a specially developed Matlab script, which allowed automating an otherwise tedious and time-consuming task.

8.2 Contact

Contact interaction was defined using a surface-to-surface, finite-sliding formulation in all FE models. In order to reduce the computational cost, contact was only defined between those surfaces of the components which were likely to interact with each other during the analysis. For built-up column 1, contact was defined between the plate sections and the flanges of the channels, while for built-up column 2, contact was defined between the web of the outer channels and the flanges of the inner channels. For built-up column 3 contact was defined between the web of the lipped channels and the flanges of the plain channels, and also between the flanges of the lipped channels and the web of the plain channels. For built-up column 4 contact was defined between the flanges of the plain channels and the webs of the lipped channels.

Interaction between the surfaces was defined as 'hard' in the normal direction using the '*Augmented Lagrange*' option as the constraint enforcement method, and as '*frictionless*' in the tangential direction.

The '*strain-free adjustment*' method was selected to eliminate any possible overclosure between the contacting surfaces due to the introduction of the measured geometric imperfections into the FE model.

8.3 Connectors

One of the main objectives of the FE modelling was to study the effect the connector behaviour has on the buckling response of CFS built-up stub columns. To achieve this, the authors looked for an accurate and efficient way to model the two different types of connectors used in the experiment:

bolts and self-drilling screws. In order to reduce the computational cost of the FE models, the body of the connectors was not explicitly modelled. Instead, a discrete approach using point-based fasteners, which employ a mesh-independent definition, was preferred. The fastening points were connected to the surfaces using CONTINUUM distributing coupling constraints between the fastening point and the neighbouring nodes on the surface.
The connectors were modelled, in turn, using MPC constraints, HINGE connectors and PLANAR connectors in order to investigate their effect on the results. MPC constraints work by eliminating the degrees of freedom of a particular node, in this case by coupling the degrees of freedom of the fasteners points on both surfaces. They have been used in the past to model the behaviour of screw connectors in CFS built-up specimens [14, 15]. On the other hand, HINGE and PLANAR connector elements impose kinematic constraints between the connected nodes, which are enforced with Lagrange multipliers [16]. HINGE connectors were used in this case to constrain all components of relative motion (CRM) between the surfaces, apart from the rotational component normal to the fastened surfaces. In the case of PLANAR connectors, two modelling sub-options were investigated. In sub-option one (referred to as '*Planar-1*') the rotational CRM normal to the surfaces, as well as the translational CRMs tangential to the surfaces were left completely unconstrained. In sub-option 2 ('*Planar-2*') the rotational CRM normal to the surface was left unconstrained, but the tangential CRMs were assigned elastic and plastic properties derived from the single lap shear tests.
The '*Hinge*' and '*Planar-1*' models can be seen as opposite ends of a spectrum. In the former, slippage at the connectors is completely prevented while in the latter infinite and unrestrained slippage is allowed. MPC constraints can be expected to lead to a similar behaviour as HINGE connectors since they also prevent slippage at the connectors.

8.4 Boundary conditions

All translational and rotational degrees of freedom of the nodes at the bottom section of the specimens were restrained. A reference point was created coinciding with the centre of gravity of the cross-section at the top end of the specimens and an MPC constraint was defined to couple all the degrees of freedom of the end section to this reference point. All rotational and translational degrees of freedom of the reference point were then restrained, apart from the translational degree of freedom in the axial direction of the specimen, which was given a value of 7 mm to simulate the compression exerted on the test specimens.

9 COMPARISON BETWEEN THE EXPERIMENTAL AND NUMERICAL RESULTS

The average ultimate loads obtained from both the experiments and the FE models are listed in *Table 3* for each set of twin columns, while *Table 4* summarizes the errors. *Table 4* shows that a good agreement was achieved between the most detailed FE models (*Planar-2*) and the experimental results for all geometries, with an average error in the ultimate load of 2.71 %, 3.57 %, 2.39 % and 5.91 % for built-up specimens SC1, SC2, SC3 and SC4, respectively. The relatively large error obtained for specimens SC4 was due to the lower ultimate load predicted for the specimens with two internal connectors (SC4-2) compared to the test results. The reason for this larger discrepancy, however, is not clear.
The *Planar-1* FE models predicted the lowest ultimate loads, underestimating the experimental capacities across all geometries. An exception to this occurred in specimens SC3, for which the *Planar-1* FE model actually predicted the highest ultimate loads. For the other geometries, the *Hinge* FE models and the *MPC* FE models were the ones that predicted the highest ultimate loads, with the *MPC* FE models predicting, on average, marginally higher ultimate loads than the *Hinge* FE models.
All FE models underestimated the ultimate capacities of specimens SC3 and SC4, which were assembled with self-drilling screws. However, contrary to expectation, the *Planar-1* FE models provided on average the closest predictions of the ultimate load for these built-up geometries.
It should be noted that, in general, the different ways in which the connectors were modelled did not have a significant effect on the ultimate capacity of the built-up stub columns under consideration.

Comparing, for each built-up specimen, the ultimate capacities given by those FE models which represent opposite ends of the spectrum, namely the *Hinge* and *Planar-1* models, only specimens SC1-3 and SC1-5 show a noticeable difference in the ultimate load (of around 20 %). For the other specimens with geometries SC1 and SC2, the differences is less than 8 %, and for geometries SC3 and SC4, the difference is less than 3 %.

Table 3. Ultimate loads obtained from experiments and FE models [kN]

	Test	MPC	Hinge	Planar-1	Planar-2
SC1-2	176.07	180.17	178.05	166.62	178.29
SC1-3	179.43	197.62	193.46	160.46	182.47
SC1-5	195.11	223.47	218.07	173.75	191.95
SC2-2	206.83	222.42	222.86	213.72	221.55
SC2-4	235.69	230.07	229.87	222.59	231.13
SC2-6	226.58	235.84	234.94	218.03	229.35
SC3-2	138.92	133.41	133.61	136.85	134.27
SC3-5	141.08	140.71	140.65	141.34	139.02
SC4-2	147.56	134.85	135.21	134.45	134.95
SC4-6	139.44	144.24	144.69	141.81	143.98

Table 4. Ultimate load comparison between experiments and FE models

	FE/Test (-)				Error (%)			
	MPC	Hinge	Planar-1	Planar-2	MPC	Hinge	Planar-1	Planar-2
SC1-2	1.025	1.013	0.948	1.014	3.37	3.64	5.18	3.91
SC1-3	1.101	1.078	0.895	1.017	10.10	7.77	10.54	1.72
SC1-5	1.146	1.119	0.891	0.985	14.64	11.87	10.88	2.71
Avg.	1.091	1.070	0.911	1.005	9.37	7.76	8.86	2.78
SC2-2	1.077	1.079	1.034	1.072	7.65	7.86	3.83	7.22
SC2-4	0.976	0.975	0.944	0.981	2.38	2.46	5.56	1.93
SC2-6	1.042	1.038	0.963	1.013	4.17	3.77	3.73	1.57
Avg.	1.032	1.031	0.980	1.022	4.73	4.70	4.37	3.57
SC3-2	0.960	0.962	0.985	0.967	3.96	3.82	1.49	3.34
SC3-5	0.998	0.997	1.002	0.986	2.44	2.44	1.69	1.44
Avg.	0.979	0.980	0.994	0.977	3.20	3.13	1.59	2.39
SC4-3	0.914	0.916	0.911	0.915	8.62	8.37	8.89	8.55
SC4-5	1.048	1.038	1.017	1.033	4.79	3.78	1.72	3.28
Avg.	0.981	0.977	0.964	0.974	6.71	6.07	5.31	5.91

10 CONCLUSIONS

An experimental and numerical programme of 20 CFS built-up stub columns with four different cross-sectional geometries and assembled using two different types of connectors is presented. All parameters that were thought to affect the buckling response of the built-up specimens, in particular the material properties, geometric imperfections and connector behaviour, were measured and incorporated into detailed FE models.

The stub column tests showed that reducing the connector spacing results in an increase in ultimate capacity which ranges from modest (up to 11%) to negligible for the range of geometries and connector spacings considered in this programme. In some cases (e.g. geometry SC4), a slight reduction in ultimate capacity was observed with reduced connector spacing.

A good agreement was achieved between the predictions of the FE models and the test results, with differences in the ultimate load of less than 6 % for all geometries tested.

Different approaches to modelling the connector behaviour were investigated in the FE models. However, it was concluded that the modelling approach (and by extension the actual connector behaviour) does not have a significant effect on the ultimate capacity of CFS built-up stub columns.

11 ACKNOWLEDGMENT

The authors gratefully acknowledge the financial support provided by the EPSRC [Grant EP/M011976/1].

REFERENCES

[1] Li Y., Shen Z., Yao X., Ma R., Liu F. "Experimental Investigation and Design Method Research on Low-Rise Cold-Formed Thin-Walled Steel Framing Buildings". *Journal of Structural Engineering* 139, pp. 818-836, 2013

[2] Dundu M. "Design Approach of Cold-formed Steel Portal Frames". *International Journal of Steel Structures* 11. No. 3, pp. 259-273, 2011

[3] Young B., Chen J. "Design of Cold-Formed Steel Built-Up Closed Sections with Intermediate Stiffeners". *Journal of Structural Engineering* 134, No. 5, pp. 727-737, 2008

[4] Zhang J.-H., Young B. "Compression tests of cold-formed steel I-shaped open sections with edge and web stiffeners". *Thin-Walled Structures* 52, pp. 1-11, 2012

[5] Lau H. H., Ting T. C. H. "An Investigation of the Compressive Strength of Cold-formed Steel Built-up I Sections". Proceedings of the Sixth International Conference on Advances in Steel Structures. ICASS'09, pp. 441-449, 2009

[6] Stone T. A., LaBoube R. A. "Behavior of cold-formed steel built-up I-sections". *Thin-Walled Structures* 43, No. 12, pp. 1805-1817, 2005

[7] Whittle J., Ramseyer C. "Buckling capacities of axially loaded, cold-formed, built-up C-channels". *Thin-Walled Structures* 47, No. 2, pp. 190-201, 2009

[8] Piyawat K., Ramseyer C., Kang T. H. "Development of an Axial Load Capacity Equation for Doubly Symmetric Built-Up Cold-Formed Sections". *Journal of Structural Engineering - ASCE* 139, No. 12, pp. 1-13, 2013

[9] C. C. Weng, Pekoz T. "Compression Tests of Cold-Formed Steel Columns". Ninth International Specialty Conference on Cold-Formed Steel Structures, No. 1, 1988

[10] Georgieva I., Schueremans L., Pyl L., Vandewalle L. "Experimental investigation of built-up double-Z members in bending and compression". *Thin-Walled Structures* 53, pp. 48-57, 2012

[11] BS EN ISO 6892-1 "Metallic materials — Tensile testing Part 1 : Method of test at ambient temperature". British Standard Institution, 2009

[12] Meza F., Becque, J., Hajirasouliha, I. "Experimental investigation of cold-formed steel built-up stub columns". 8th International Conference on Advances in Steel Structures, Lisbon, Portugal, Paper 36, 2015

[13] Dubina D., Ungureanu V., Landolfo R. "Design of Cold-formed Steel Structures – Eurocode 3: Design of Steel Structures Part 1-3: Design of Cold-formed Steel Structures". ECCS – European Convention for Constructional Steelwork, 2012

[14] Anapayan T., Mahendran M. "Numerical modelling and design of LiteSteel Beams subject to lateral buckling". *Journal of Constructional Steel Research* 70, pp. 51-64, 2012

[15] Zhang J., Young B. "Numerical investigation and design of cold-formed steel built-up open section columns with longitudinal stiffeners". *Thin Walled Structures* 89, pp. 178-191, 2015

[16] Dassault Systèmes, "Abaqus Analysis User's Guide Volume IV", version 6.14, Dassault Systèmes Simulia Corp., Providence, RI, USA, 2014